Journal of Engineering Science and Technology
Vol. 13, No. 4 (2018) 1016 - 1033
© School of Engineering, Taylor's University

ENHANCING LOW VOLTAGE RIDE THROUGH CAPABILITY IN UTILITY GRID CONNECTED SINGLE PHASE SOLAR PHOTOVOLTAIC SYSTEM

RINI ANN JERIN A.*, MANU THOMAS, PALANISAMY K., UMASHANKAR S.

School of Electrical Engineering, VIT University, Old Katpadi Road, Vellore,Tamil Nadu, India, 632014
*Corresponding Author: riniannjerin@gmail.com

Abstract

The steady rise in utility grid penetration of single phase solar photovoltaic system has contributed to the mandatory requirement of Low Voltage Ride-through (LVRT) capability. LVRT capability provides stable grid integration during transient conditions. A seamless LVRT capability operation in a single phase photovoltaic system using peak value based fault detection and Orthogonal Signal Generation (OSG) based voltage sag detection is conducted. In this paper, two controllers are employed for two different operations. The PQ theory controller is used for power control operation and Proportional–Resonant (PR) with Harmonic Compensation (HC) controller is used for current control operation in LVRT. MATLAB/Simulink verifies the LVRT operation mode as per the grid code requirements to ride through voltage sag during fault condition. It is observed that the system is in operation during transient conditions and provides reactive support to ride through the fault.

Keywords: Low voltage ride-through, Single phase photovoltaic, Proportional resonant (PR) control, Harmonic compensator control, Renewable energy, Solar energy.

1. Introduction

The recent growth in solar technology and cost reduction in solar panels has led to a rapid increase in the installation of solar photovoltaic systems and integration of utility grid [1, 2]. The sudden increase in renewable energy integration was not assumed during the planning of conventional utility grid and therefore the grid codes for renewable penetration requires modification when connected to the utility grid [3, 4]. Low Voltage Ride Through (LVRT) capability in wind energy

Nomenclatures

dI	Change in current, A
dP	Change in power, W
dV	Change in voltage, V
$G_{HC}(s)$	Transfer functions for Harmonic compensator
$G_{PR}(s)$	Transfer functions for PR controller
$G_p(s)$	Proportional integral (PI) controller gain for active power control
$G_q(s)$	Proportional integral (PI) controller gain for reactive power control
I	Current, A
$I_{g\alpha}^*$, $I_{g\beta}^*$	Reference current signals in α, β reference frame
I_{max}	Maximum power point tracking current from PV array, A
I_N	Nominal inverter current, A
I_p	Active current, A
I_q	Reactive current, A
K	Temperature, ^oC
k_{ih}	Gain for harmonic compensator
k_p ,k_i	Gains for PR controller
P	Power, or active power, W
Q	Reactive power, Var
R_L	Load resistance, Ohm
V	Voltage, V
V_g	Instantaneous grid voltage, V
$V_{g\alpha}^*$, $V_{g\beta}^*$	Reference voltage signals in α, β reference frame
V_{mmp}	Voltage at the maximum power point of the curve, V
V_N	Nominal grid voltage, V
V_p	Voltage at pink point in curve, V

Abbreviations

AF	Adaptive Filter
CERC	Central Electricity Regulatory Commission
DC	Direct Current
EPLL	Enhanced Phase Locked Loop
HC	Harmonic Compensator
INC	Incremental Conductance
LVRT	Low Voltage Ride Through
MPPT	Maximum Power Point tracking
OSG	Orthogonal Signal Generator
P&O	Perturb and Observe
PCC	Point of Common Coupling
PD	Phase Detector
PI	Proportional Integral
PLL	Phase Locked Loop
PQ	p-q Power Components theory
PR	Proportional Resonant
PV	Photovoltaic
RMS	Root Mean square
SOGI-PLL	Second Order Generalized Integrator PLL

had been established previously due to the penetration of high capacity large wind turbines. Similarly there have been great advancements in the solar photovoltaic inverter technology in the recent past to improve its efficiency. Therefore large scale installations of single phase solar photovoltaic systems have necessitated the requirements for LVRT capability. The LVRT capability is in order to sustain the operation of solar power generation during transient conditions without the sudden tripping of solar generation from the grid. This will avoid the sudden loss of power during transient conditions and also will help in supporting the grid by providing reactive power support. The LVRT capability will support the grid during adverse transient conditions like during fault and also support the grid to return back to the nominal condition by providing the reactive power support [5]. The LVRT capability will promote the high penetration of solar photovoltaic system into the grid and the use of clean renewable energy [6-10].

At present, the solar Photovoltaic (PV) inverters run below their rated current converting DC solar power to AC active power for over 90% of their run time. This unused capacity is put to use to produce reactive power during faulty conditions in the grid to provide LVRT. Very few grid codes and articles deal with the LVRT capability in PV systems connected to low-level grid like the single phase PV systems. As a solution for this problem, the utility operators and other standardization agencies are trying to introduce Low Voltage Ride through (LVRT) capability requirements in PV inverters that are integrated to the grid, similar to the grid codes which are already present in wind energy systems [11]. European countries like Spain and Germany recently introduced PV plant grid connection standards. Italy has issued grid codes exclusively for PV integration. UK, France and Czech Republic are going to implement similar codes to their distribution network as per the reports of European Commission. They also need to follow the ENTSO network codes. Recently in US, the North American Electric Reliability Corporation has accepted the PRC-024-1 [12], which describes the LVRT curves while in Canada, the Hydro-Quebec standard is followed from 2009. LVRT in terms of wind energy plants reduces the power loss incurred due to faults. [13-17].

In case of PV systems, it's more elaborate and expected to stay connected to grid as per grid code period during faults up to 0.9 pu to 0.2 pu of the nominal grid voltage [18]. It is also required to feed reactive power during faults to support grid recovery. It should resume the active power support immediately after the fault is removed. In [19], the LVRT capability is tested with three different aspects such as reactive power injection, current stresses and leakage current rejection in single phase transformer-less PV inverter. The same system is tested with different irradiance and temperature conditions for testing its reliability in [20]. In [21], a new power control method is developed for improving the system efficiency during the fault condition in existing grid requirements. The design of filters and developing the advanced synchronizing methods for grid connected PV system is the crucial part to determine the efficiency of the system which is discussed in [22-24]. The MPPT tracking in solar helps in obtaining maximum energy yield [25, 26], in this paper Incremental Conductance (INC) method is used for MPPT tracking. The INC method operates such that when the ratio of change of output conductance is equal to negative output conductance, the PV will operate at the maximum power point. In this method the terminal voltage of the array is always adjusted according to the MPP.

Hence, this paper mainly focuses on the LVRT capability in a single phase photovoltaic system using peak value based fault detection and Orthogonal Signal Generation (OSG) based voltage sag detection is conducted. Also, two different controllers such as PQ theory controller and Proportional–Resonant (PR) with Harmonic Compensation (HC) controller are used for power control and current control operation respectively. Also, India which is fast moving in the forum of renewable power generation and utilization is also trying to adopt LVRT grid codes for large scale PV systems connected to the transmission or distribution grid [27]. Possible solutions for single-phase applications are based on the single-phase *PQ* theory, instantaneous power control, or the droop control concept [28-30]. Since LVRT in solar is a upcoming topic the new explorations on control methods need to verified.

The organization of this article as follows: The LVRT operation of a single phase grid-tied solar PV system as per the new grid codes established is carried out and the introduction has been discussed in Section 1. The Section 2 discusses the grid code standards established for LVRT capability of Solar PV system, Section 3 discusses the system configuration for the Solar PV system and the sag detection using peak-value based sag detection and a quarter cycle delay based Orthogonal Signal Generator (OSG) system for generation of orthogonal components which is used for sag detection and power control. Section 4 shows the results of the MATLAB based simulation which shows satisfactory performance of the LVRT operation as per the grid codes. Section 5 concludes and shows that the system is useful for providing a seamless LVRT operation of the solar PV by providing the required reactive power support and operating without tripping.

2. Grid standards for LVRT Capability for Solar PV Systems

The analytical methods E. ON grid codes [31] established for wind turbines are used as a reference to implement the LVRT control in solar PV in this paper. The LVRT grid codes and the anti-islanding requirements for small PV units defined by IEC for various countries are given in Fig. 1 as given in [20]. Voltage control through reactive power control is provided during voltage sag is allowed by injecting the reactive power into the distribution grid. Therefore, during severe voltage sag conditions, the system disables the active power but has to fully inject the reactive power.

In order to keep the voltage at desirable levels, sufficient reactive power injection is made possible as the system is operated under partial loading conditions. The reactive power delivered depends on the apparent power of the inverter. The reactive power support based on German grid codes done should also satisfy the minimum power factor requirement and is given in Fig. 2 [21].

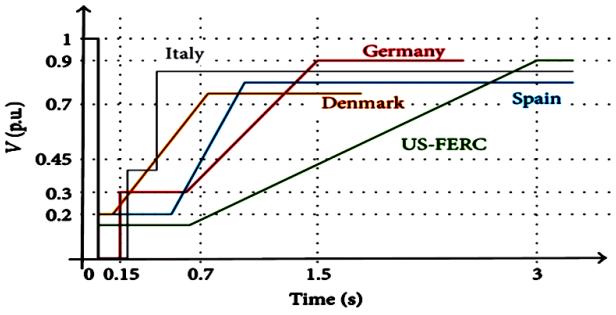

Fig. 1.LVRT standards for various countries [20].

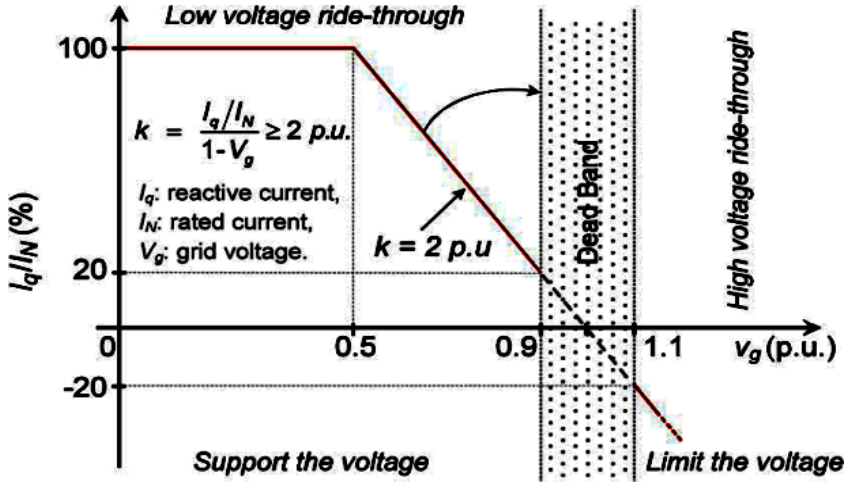

Fig. 2. Reactive current requirement [21].

Based on German grid code, the PV system is required to stay connected for a voltage drop up to zero for duration of 0.15 s, which has to be followed by voltage recovery to the 90% of the nominal grid voltage at the point of common coupling (PCC) for duration of 1.5 s. The reactive power injection is based on the constraint as given in Eq. (1). The voltage support through the injection of reactive current is required outside voltage dead-band of ±10% as described in Eq. (2). Restoration of active power is essential to maintain the frequency limits based on the peak value as described in Eq. (3). Similarly, the LVRT requirements vary in each country based on their grid codes [32].

$$I_p{}^2 + I_q{}^2 = I_N{}^2 \leq I_{max} \tag{1}$$

$$I_q = \begin{cases} deadband, \ \ 0.9 \leq \frac{V_g}{V_N} \leq 1 \\ 2 \times \frac{V_g}{V_N} \times I_N, 0.5 < \frac{V_g}{V_N} < 0.9 \\ I_N, \frac{V_g}{V_N} \leq 0.5 \end{cases} \tag{2}$$

$$I_p = \begin{cases} I_m, \ \ 0.9 \leq \frac{V_g}{V_N} \leq 1 \\ \sqrt{I_N{}^2 - (2 \times \frac{V_g}{V_N} \times I_N)^2}, 0.5 < \frac{V_g}{V_N} < 0.9 \\ 0, \ \frac{V_g}{V_N} \leq 0.5 \end{cases} \tag{3}$$

where I_q and I_p are the reactive and active currents required by the grid. V_g,V_N,I_N,I_{max} are the Instantaneous grid voltage, nominal grid voltage, nominal inverter current and MPP current from PV array respectively.

The LVRT grid codes in India also states that [33] the LVRT requirement is necessary to maintain the stability of the grid. Therefore LVRT capability in solar

inverters has been include in the regulation. As per Section 30 in Central Electricity Regulatory Commission (CERC), LVRT provision is mandatory for all solar generators connected at the voltage level of 11 kV and above. CERC has issued direction for meeting requirements of LVRT in case of solar generating stations whose bidding process has not yet commenced as of 05.01.2016.

2.1. System configuration

Single-phase PV system can be configured in single stage or dual stage structure. The dual stage configuration has an added boost stage to regulate the PV array output to harness the maximum power. There are different algorithms for Maximum Power Point Tracking (MPPT) like Perturbation and Observation (P&O) or the Incremental Conductance (INC) methods. These algorithms try to adjust the operating point voltage in the direction of maximum power output. In the second stage there is grid connected inverter with a basic dual loop control; an outer DC link voltage or power control loop and an inner current control loop. The dc-link capacitor voltage is regulated by the voltage control loop, thereby controlling the power delivery to the grid. The inner current loop maintains the power quality according to prescribed standards [34].

Grid Synchronization includes the proper tracking of phase and amplitude of the grid voltage and current. This is usually done using Phase Locked Loop (PLL) based method or by mathematical analysis. The single phase PLL is differentiated by the Phase Detector (PD) configuration [35]. Park's transformation on the Orthogonal Signal Generation (OSG) system is used for extracting phase error in PLL [36]. As per fundamental frequency of the input grid voltage, *T/4* delay PLL can introduce a phase shift of $\pi/2$ rad which is the simplest method. Or else an Adaptive Filter (AF) can be utilized to achieve the same which can adjust the output with respect to the error feedback. Advanced PLL technique includes Enhanced PLL (EPLL) and Second Order Generalized Integrator based PLL (SOGI-PLL) which are combination of Adaptive Filters and sinusoidal multiplier or OSG system respectively [35]. EPLL operates by locking the output voltage signal magnitude and also the phase. The advantage of SOGI-PLL is the better reduction of harmonics. PLL-based algorithms are preferred options due to the robustness and are frequency adaptive to grid variations.

2.1.1. Incremental conductance based MPPT in solar PV

The equation for implementing the INC algorithm can be easily obtained from the basic power equation. The equation for power is given as

$$P = V I \tag{4}$$

Differentiating the above equation with respect to voltage yields,

$$dP / dV = d(V*I) / dV \tag{5}$$

$$P = V I \tag{6}$$

The condition for the maximum power point tracking is that the slope dP / dV should be equal to zero. Substituting in the above equation,

$$dI / dV = - (I/V) \tag{7}$$

Also, the following conditions have helped to track the maximum power point based on the INC algorithm.

$$dP/dV > 0, \text{ then } V_p < V_{mmp} \quad (8)$$

$$dP/dV = 0, \text{ then } V_p = V_{mmp} \quad (9)$$

$$dP/dV < 0, \text{ then } V_p > V_{mmp} \quad (10)$$

The above equations are implemented in Matlab Simulink to track the maximum Power point of the PV panel. Figure 3 shows that when Eq. (9) is true, the MPPT is tracked correctly and the PV value at the pink point is figured out. This method provides reduced number of oscillations around the MPP and stable operation. Figure 4 shows the power vs. voltage curve of the solar PV system. Figure 5 shows the Simulink model of the PV system implemented.

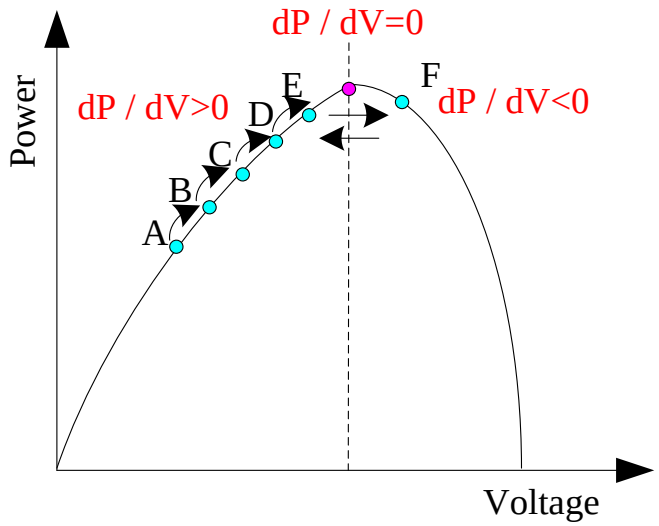

Fig. 3. Incremental conductance method for MPPT.

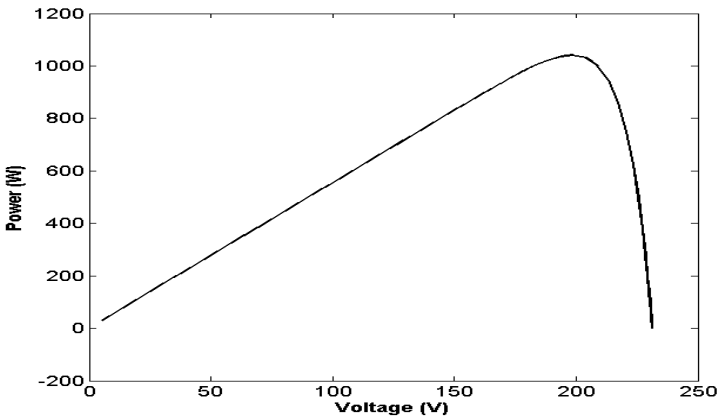

Fig. 4 P-V curve for PV array.

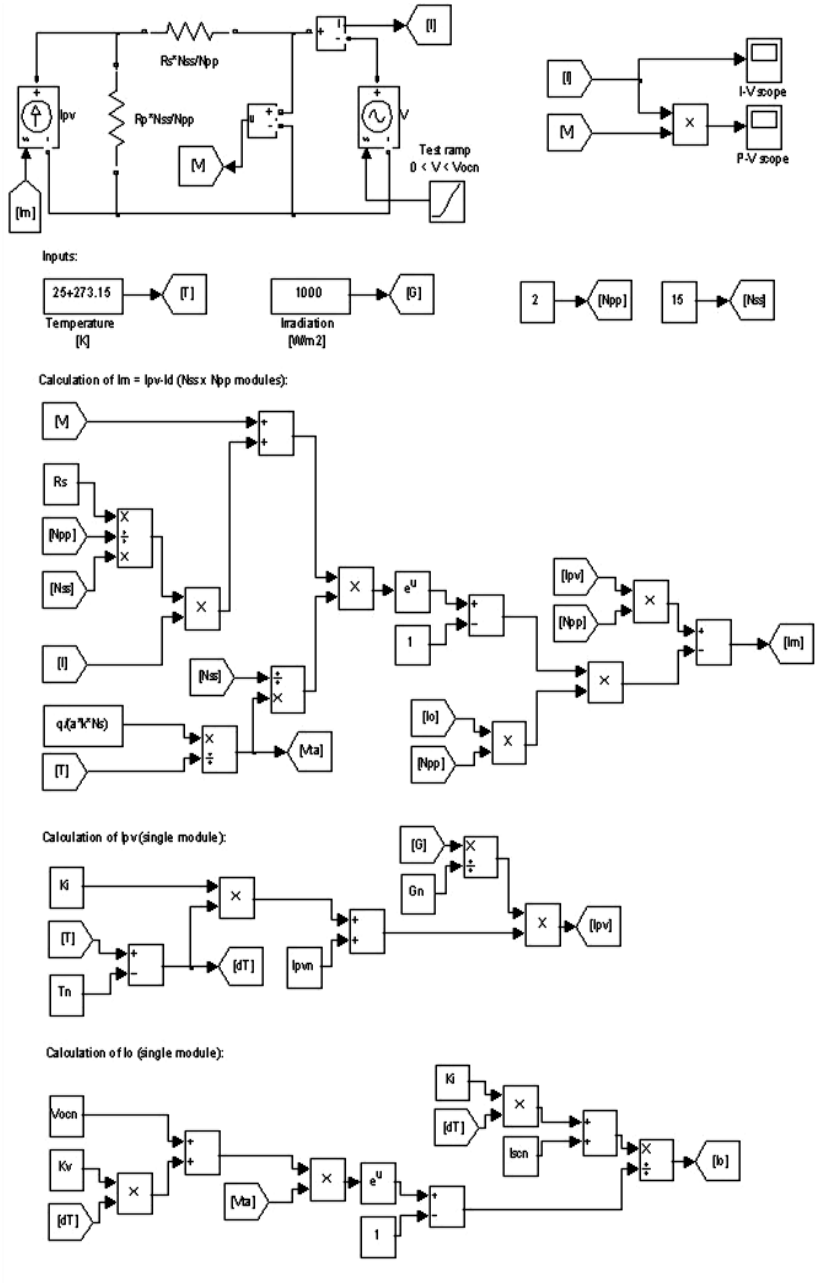

Fig. 5. Simulink model for photovoltaic system.

2.2. Control of PV System

2.2.1. Sag detection unit

RMS Value Calculation Method [35] which is calculated for continuous samples of input voltage data. As the number of samples increases the accuracy also

increases. It gives one time period old average value, not the instantaneous value. The error between the required instantaneous voltage and the actual value is calculated in the Missing Voltage method [36]. The required value can be found easily by using the pre-event voltage value and extrapolating to get the values during the event just as in case of a PLL operation. Peak Value Evaluation Method is shown in [35]. The single-phase line-to-neutral voltage is obtained from sensor measurement and orthogonal signal is generated by giving a 90 degree phase shift. These orthogonal components of voltage are squared and the square root is taken to give the peak value.

2.2.2. Power reference calculation

A power profile is considered for various inverter control modes to find out the reference active and reactive powers. Maximum active power should be supplied to the grid during the normal inverter operation. So the active power reference is set as P_{PV}, which is equal to the Power output of the PV array maximized by the MPPT algorithm. The reactive power reference is set as zero. During LVRT operation, the power references are found in accordance to the LVRT standards as mentioned in the previous grid standard section. There are various inverter current limitation strategies like constant peak current strategy, constant average active power strategy and constant active current strategy. In this paper, a constant peak current strategy is used.

2.2.3. Sag generator circuit

For the simulation of voltage fault and its consequent sag in voltage magnitude, a sag generation circuit is added in the grid. A series low impedance resistance is switched during the required fault period using switch S_1. A load resistance, R_L is also added during fault to limit the short-circuit effect during inverter upstream. With regular operation switch S_1 is closed and switch S_2 is open.

2.2.4. Reference current generation

The outer loop regulates voltage amplitude and grid frequency. A current reference is subsequently generated to be utilized in the inner loop as shown in Fig. 6. In this paper, single-phase PQ theory [37, 38] is used to generate grid current reference. This is generated by controlling the averaged active power and reactive power. The power references are given by the power profile for various modes.

The voltage control generates the current reference as shown in the following equation.

$$\begin{bmatrix} I_{g\alpha}^{*} \\ I_{g\beta}^{*} \end{bmatrix} = \frac{1}{V_{g\alpha}^{2} + V_{g\beta}^{2}} \begin{bmatrix} V_{g\alpha} & V_{g\beta} \\ V_{g\beta} & -V_{g\alpha} \end{bmatrix} \begin{bmatrix} G_p(s)(P - P^{*}) \\ G_q(s)(Q - Q^{*}) \end{bmatrix} \begin{bmatrix} I_{g\alpha}^{*} \\ I_{g\beta}^{*} \end{bmatrix} \tag{11}$$

where "*" represents the reference signals, $G_p(s)$ and $G_q(s)$ are the proportional integral (PI) controller gains for active and reactive power controller as shown in equation (4) respectively. This scheme doesn't need to have Park and Inverse Park transformations. This scheme is effective to generate current reference with much ease. There are other control schemes mentioned in literatures [39] like the droop based power control method.

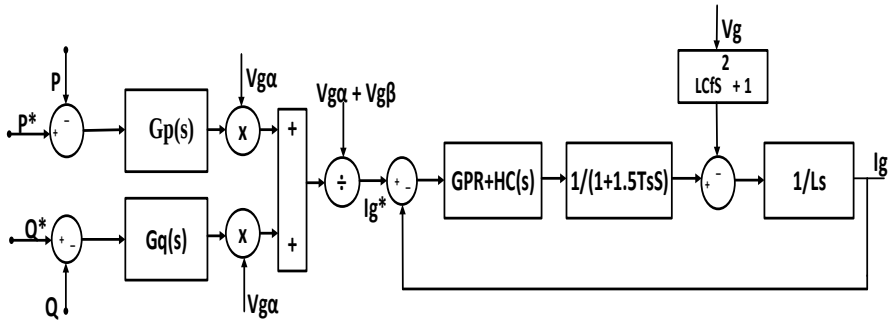

Fig. 6. Current reference generation using PQ theory

2.2.5. Current loop control

The power quality standard of the injected power to the grid is ensured by the current controller. The effective design of filters with correct damping resistance and proper selection of harmonic compensators are essential to maintain the power quality. These factors have to be taken into consideration while designing a current controller.

The choice of reference frame is important while designing a current controller. $\alpha - \beta$ and $d - q$ are the commonly used reference frames. Basic PI based controller needs $d - q$ parameters. As Park and Inverse Parks transformations are utilized, the $d - q$ frame implementation becomes comparatively difficult. The gain of the Proportional Resonant (PR) control realized in the $\alpha\beta$ reference frame is shown in the following equations.

$$G_{PR}(s) = k_p + \frac{k_i s}{s^2 + \omega_0^2} \tag{12}$$

$$G_{HC}(s) = \frac{k_{ih} s}{s^2 + (h\omega_0)^2} \tag{13}$$

where, $G_{PR}(s)$ and $G_{HC}(s)$ are the transfer functions for PR controller and Harmonic compensator as shown in equation (5) and (6) respectively. k_p , k_i are the gains for PR controller while k_{ih} is the gain for Harmonic compensator.With the change in the operation mode (MPPT or LVRT) the current harmonic also changes. The current harmonics is also affected with change in power factor and voltage levels. The transient responses and harmonic attenuation capabilities of the above mentioned single phase controllers are not good enough during dynamic operating conditions. The DC link capacitor voltage may oscillate at double rate of the grid frequency which can subsequently introduce even order harmonics to the injected current which may increase during the LVRT operation mode. Therefore, it shows that a single PR or DB controller cannot handle the condition. Hence, a combination of PR and Harmonic compensator (HC) is involved to obtain a better control.

3. Simulation Results

The PV system with the proposed control is implemented using Matlab/Simulink. The PV array gives maximum output of 1100 W at an output voltage 235 V and

corresponding current of 4.7 A. INC algorithm is used to track the maximum output power of the PV system. The DC link capacitor voltage is regulated at 400 V. Grid fault of 0.35 p.u. at T = 0.3 s occurs and the voltage sag lasts for about 200 ms and the simulation parameters involved are given in Table 1.

The conditions in taken into account for the implementation of this proposed method is as follows:

- During fault condition, the MPPT is disabled and the control is switched to grid fault operation mode.
- In the LVRT mode, the system injects reactive current and limits active power output to prevent the inverter from over-current.
- After clearing fault the system resumes normal operation and again tracks the maximum output power of the PV panels.
- Maximum active power should be supplied to the grid during the normal inverter operation.
- During LVRT operation, reactive power support has to be offered. Active power limitation is carried out to avoid over-current shutdown of the PV inverter.

P-V curve of the solar array is shown in Fig. 4 Flowchart for power reference generation during various modes is as shown in Fig. 7. The appropriate formulas for generating the curves are discussed in [40-43]. The grid voltage during LVRT operation is shown in Fig. 8 and grid current is shown in Fig. 9. The DC power output of the boost converter is shown in Fig. 10. Also, the active and reactive power during LVRT operation mode is shown in Fig. 11.

Table 1. PV system parameters.

System Parameters	Values
Nominal Grid Voltage, V_n	325 V
Grid Frequency, f	50 Hz
LC Filter, L_f	3.7 mH
LC Filter, C_f	2.70 µH
Transformer Leakage, Resistance, R_T	0.02 Ω
Transformer Leakage,Reactance, L_T	4mH
Sag Generator, R_s	19.4 Ω
Sag Generator,R_L	21 Ω
Active Power Controller, $k_{pp,}$ k_{pi}	6.2, 1.6
Reactive Power Controller, k_{Qp}, k_{Qi}	1, 52
PR Controller, k_p, k_i	22,2000
HC Controller,k_{Hi}, k_{Hih}, h=3,5,7	5000

The THD analysis is done through FFT analysis for grid voltage during MPPT mode as shown in Fig. 12 which shows a THD of 4.96%. Grid voltage during LVRT mode has 5.59% as shown in Fig. 13. FFT analysis for Grid Current during MPPT mode has 4.22% as shown in Fig. 14 and for Grid Current during LVRT mode has 4.83% as shown in Fig. 15. This THD comparison is also shown in Table 2. Also, a detailed comparison of the single phase PV system operation is discussed in Table 3 according to the grid parameters. The results clearly show that the LVRT operation is under acceptable limits and gives a satisfactory performance. This study has enabled the analysis of the system under LVRT condition and can be further improved with advanced control schemes.

Table 2. Grid voltage and current THD for various modes of operation

System Parameters	MPPT mode	LVRT mode
Voltage, V	4.91	5.59
Current, A	4.08	4.83

Table 3. Comparison of MPPT and LVRT modes based on grid parameters

PV System Parameters	MPPT mode	LVRT mode
Solar PV output, *Ppv*	1100 W	480 W
Voltage supplied, *Vg*	235 V	200 V
Active Power supplied, *P*	1050 W	460 W
Reactive Power supplied, *Q*	20 Var	440 Var

The simulation results illustrate the versatility of a PV inverter in supporting grid. The power control method based on the P-Q theory acts during fault condition in grid to supply the reactive power but causes some oscillations in voltage and current output post-fault condition. There ramp rate of the voltage profile is not linear and can be improved with better tuning of gain values of the control. The proper detection of voltage sag by improving the voltage and current controllers will ensure a smooth transition from LVRT to normal operation mode. Instantaneous shifting from LVRT mode to normal operation mode is possible by utilizing fast detection schemes. However, the control utilized ensures the operation of grid-tied solar PV as per the grid code standards.

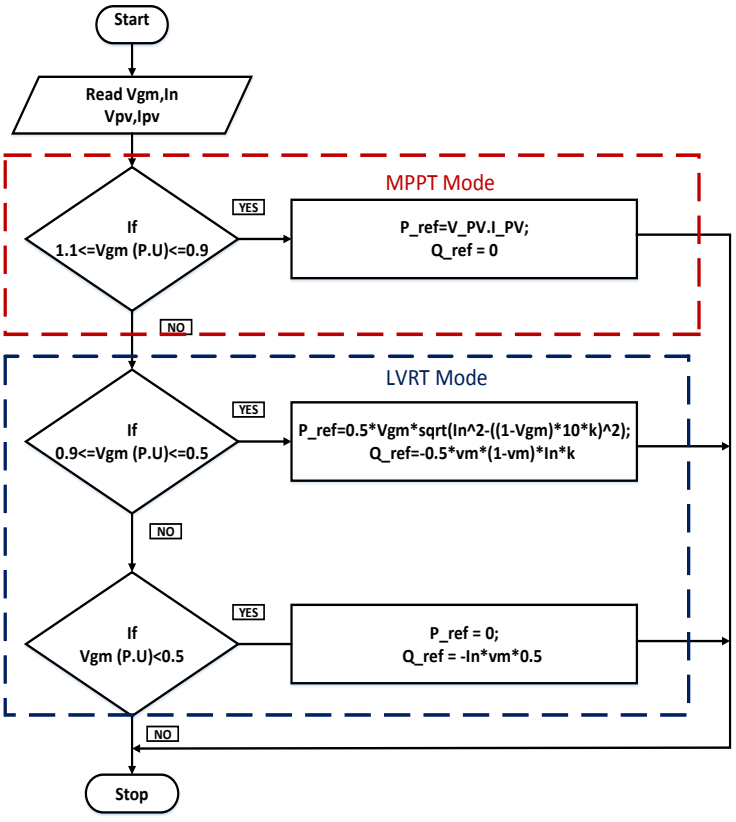

Fig. 7. Flowchart for power reference generation during various modes.

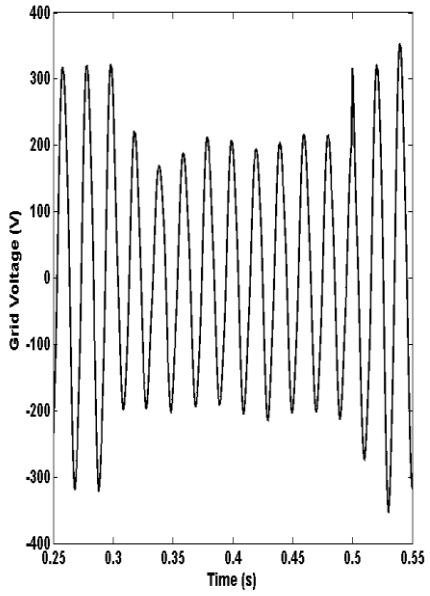

Fig. 8. Grid voltage during LVRT operation of voltage sag 0.35 pu during 0.3 s for 200 ms.

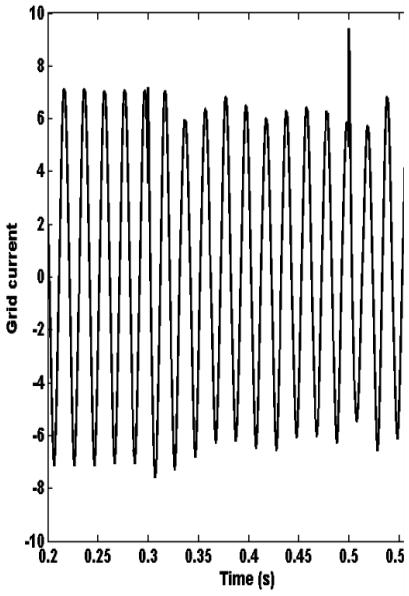

Fig. 9. Grid current during LVRT operation of voltage sag 0.35 pu during 0.3 s for 200 ms.

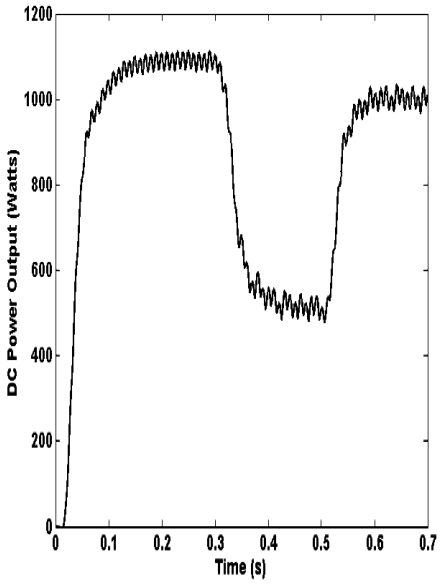

Fig. 10. DC power output for Boost converter.

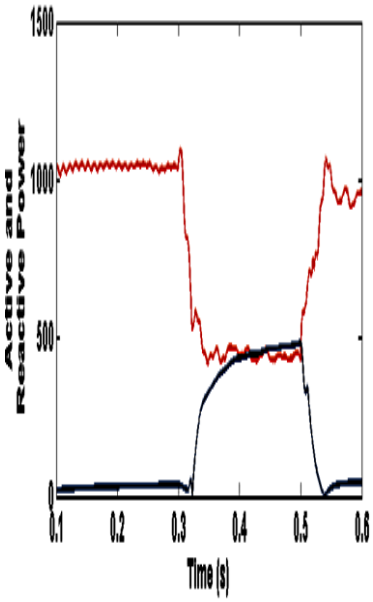

Fig. 11. Active and Reactive power of voltage sag 0.35 pu during 0.3 s for 200 ms during LVRT operation.

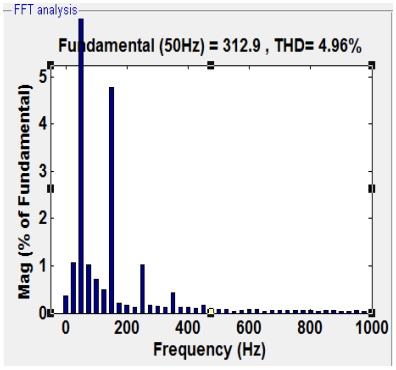

Fig. 12. FFT analysis for grid voltage during MPPT mode.

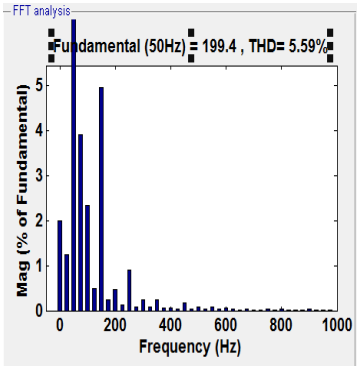

Fig. 13. FFT analysis for Grid voltage during LVRT mode.

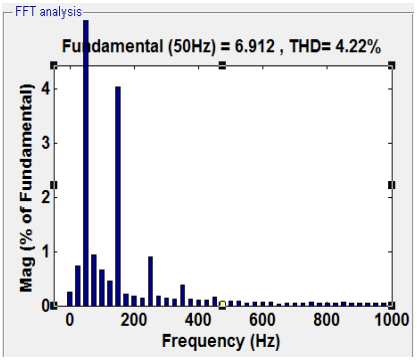

Fig. 14. FFT analysis for Grid Current during MPPT mode.

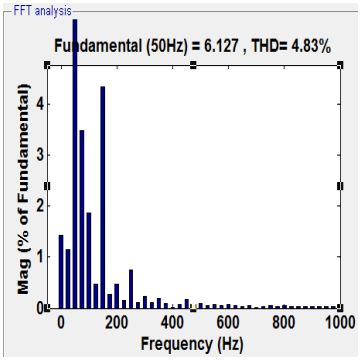

Fig. 15. FFT analysis for Grid Current during LVRT mode.

It can be concluded that the future single-phase grid-connected PV systems are ready to be more active and more "smart" in the regulation of power grid. Like the conventional generation systems, the single-phase PV systems can also offer some ancillary service in the presence of an abnormal grid condition. However, the performance is dependent on the grid detection and control methods. In this paper, the overall control strategy for single-phase PV systems in the grid faulty mode operation is demonstrated based on the grid requirements defined for three-phase wind power systems as it is expected that they will be the basic requirements for single-phase PV systems. Nevertheless, for different applications, the presented benchmarking result provides a convenient way to select appropriate devices of those inverters. The test results have verified the effectiveness of the single-phase *PQ* control method under grid faults and the constant peak current control strategy for reactive power injection.

4. Conclusions

With the fast development of distributed power generations, stability and security have attracted extensive attention in the recent years. As a representative of clean

energies, Photovoltaic (PV) systems have been installed extensively worldwide. The ride through capability during voltage sag conditions in grid due to fault is demonstrated for grid-tied single phase PV. The control utilized ensures the stable performance of the PV system and the reliability of grid. Peak value based fault detection is utilized and a single phase P-Q theory is used to generate current reference and an enhanced current control operation done using PR+HC control. In normal operation, active power is generated and during LVRT operation PV inverter injects reactive current into power grid to ride through the fault. Active power limitation is carried out to avoid over-current shutdown of the PV inverter. Therefore, the reliability of PV systems when integrated to grid in large-scale is preserved through this LVRT control operation. Simulation results are presented, which verifies that the LVRT methods can help the PV systems to temporarily ride-through the grid low voltage faults. However the performance is dependent on the grid detection and control methods.

References

1. Ding, M.; Xu, Z.; Wang, W.; Wang, X.; Song, Y.; and Chen, D. (2016). A review on China′ s large-scale PV integration: Progress, challenges and recommendations. *Renewable and Sustainable Energy Reviews*, 53, 639-652.
2. Rodrigues, E.M.G.; Osório, G.J.; Godina, R.; Bizuayehu, A.W.; Lujano-Rojas, J. M.; and Catalão, J. P. S. (2016). Grid code reinforcements for deeper renewable generation in insular energy systems. *Renewable and Sustainable Energy Reviews*, 53, 163-177.
3. Sasidharan, N.; and Singh, J.G. (2017). A resilient DC community grid with real time ancillary services management. *Sustainable Cities and Society*, 28, 367-386.
4. Arulkumar, K.; Vijayakumar, D.; and Palanisamy, K. (2016). Recent advances and control techniques in grid connected PV system - A review. *International Journal of Renewable Energy Research*, 6(3), 1037-1049.
5. Saad, N.H.; El-Sattar, A. A.; and Mansour, A. E. A. M. (2016). Improved particle swarm optimization for photovoltaic system connected to the grid with low voltage ride through capability. *Renewable Energy*, 85, 181-194.
6. Adouni, A.; Chariag, D.; Diallo, D.; Hamed, M. B.; and Sbita, L. (2016). FDI based on Artificial Neural Network for Low-Voltage-Ride-Through in DFIG-based Wind Turbine. *ISA transactions*, 64, 353-364.
7. Rini Ann Jerin, A.; Palanisamy, K.; and Umashankar, S. (2017). Improved fault ride through capability of DFIG based wind turbines using synchronous reference frame control based dynamic voltage restorer. *ISA Transactions*, 70, 465-474.
8. Rini Ann Jerin, A.; Palanisamy, K.; Umashankar, S.; and Sanjeevikumar, P. (2017). Improved Fault Ride Through Capability in DFIG based Wind Turbines using Dynamic Voltage Restorer with Combined Feed-Forward and Feed-Back Control, *IEEE Access*, 5, 20494-20500.
9. Rini Ann Jerin, A.; Prabaharan, N.; Palanisamy, K.; and Umashankar, S. (2017). FRT capability in DFIG based wind turbines using DVR with CFFFB control. *Energy Procedia*, 138, 1184-1189.

10. Rini Ann Jerin, A.; Palanisamy, K..; Umashankar, S.; and Sanjeevikumar, P. (2016). Comparative analysis of feed-forward and synchronous reference frame control based dynamic voltage restorer. *Lecture Notes in Electrical Engineering*, 436, 411-420.
11. Kovanen, K. O. (2013). Photovoltaics and power distribution. *Renewable Energy Focus*, 14(3), 20-21.
12. Shivashankar, S.; Mekhilef, S.; Mokhlis, H.; and Karimi, M. (2016). Mitigating methods of power fluctuation of photovoltaic (PV) sources–A review. *Renewable and Sustainable Energy Reviews*, 59, 1170-1184.
13. Blaabjerg, F.; Chen, Z.; and Kjaer, S. B. (2004). Power electronics as efficient interface in dispersed power generation systems. *IEEE transactions on power electronics*, 19(5), 1184-1194.
14. Prabaharan, N.; Rini Ann Jerin, A.; and Palanisamy, K. (2017). Integration of single phase reduced switch multilevel inverter topology for grid connected photovoltaic system, *Energy Procedia*, 138, 1177-1183.
15. Prabaharan, N.; Palanisamy, K.; and Rini Ann Jerin, A. (2015). Asymmetric multilevel inverter structure with hybrid PWM strategy. *International Journal of Applied Engineering Research*, 10(55), 2672-2676.
16. Rini Ann Jerin, A.; Jayakumar, J.; Prabaharan, N.; Palanisamy, K.; Umashankar, S.; and Thirumoorthy, A.D. (2015). Frequency control of a stand- alone hybrid wind and solar based distributed generation system through optimized energy storage. *International Journal of Applied Engineering Research*, 10(10), 9982-9988.
17. Rini Ann Jerin, A.; Palanisamy, K.; Umashankar, S.; and Thirumoorthy, A. D. (2016). Power quality improvement of grid connected wind farms through voltage restoration using dynamic voltage restorer. *International Journal of Renewable Energy Research (IJRER)*, 6(1), 1316-1323.
18. Blaabjerg, F.; Teodorescu, R.; Liserre, M.; and Timbus, A. V. (2006). Overview of control and grid synchronization for distributed power generation systems. *IEEE Transactions on industrial electronics*, 53(5), 1398-1409.
19. Yang, Y.; Blaabjerg, F.; and Wang, H. (2014). Low-voltage ride-through of single-phase transformerless photovoltaic inverters. *IEEE Transactions on Industry Applications*, 50(3), 1942-1952.
20. Yang, Y.; and Blaabjerg, F. (2013). Low-voltage ride-through capability of a single-stage single-phase photovoltaic system connected to the low-voltage grid. *International Journal of Photoenergy*, 2013, 1-9.
21. Yang, Y.; Chen, W.; and Blaabjerg, F. (2014). Advanced control of photovoltaic and wind turbines power systems. *Advanced and Intelligent Control in Power Electronics and Drives*. 41-89.
22. Pena-Alzola, R.; Liserre, M.; Blaabjerg, F.; Ordonez, M.; and Yang, Y. (2014). LCL-filter design for robust active damping in grid-connected converters. *IEEE Transactions on Industrial Informatics*, 10(4), 2192-2203.
23. Hadjidemetriou, L.; Kyriakides, E.; Yang, Y.; and Blaabjerg, F. (2016). A synchronization method for single-phase grid-tied inverters. *IEEE Transactions on Power Electronics*, 31(3), 2139-2149.

24. Yang, Y.; and Blaabjerg, F. (2012, June). Synchronization in single-phase grid-connected photovoltaic systems under grid faults. *Power Electronics for Distributed Generation Systems (PEDG), 2012 3rd IEEE International Symposium*, pp. 476-482.
25. Khadidja, S.; Mountassar, M.; and M'hamed, B. (2017). Comparative study of incremental conductance and perturb & observe MPPT methods for photovoltaic system. In *Green Energy Conversion Systems (GECS), 2017 International Conference*, pp. 1-6.
26. Sharma, D.K.; and Purohit, G. (2014). Maximum power angle (MPA) based maximum power point tracking (MPPT) technique for efficiency optimization of solar PV system. *International Journal of Renewable Energy Research (IJRER)*, 4(3), 810-815.
27. Riza, D.F.A.; Gilani, S.I.U.H.; and Aris, M.S. (2015). Standalone photovoltaic systems sizing optimization using design space approach: case study for residential lighting load. *Journal of Engineering Science and Technology* (*JESTEC*), 10(7), 943-957.
28. Mastromauro, R.A.; Liserre, M.; Kerekes, T.; and Dell'Aquila, A. (2009). A single-phase voltage-controlled grid-connected photovoltaic system with power quality conditioner functionality. *IEEE Transactions on Industrial Electronics*, 56(11), 4436-4444.
29. Dasgupta, S.; Sahoo, S.K.; and Panda, S.K. (2011). Single-phase inverter control techniques for interfacing renewable energy sources with microgrid - Part I: Parallel-connected inverter topology with active and reactive power flow control along with grid current shaping. *IEEE Transactions on Power Electronics*, 26(3), 717-731.
30. Khajehoddin, S. A.; Karimi-Ghartemani, M.; Bakhshai, A.; and Jain, P. (2013). A power control method with simple structure and fast dynamic response for single-phase grid-connected DG systems. *IEEE Transactions on Power Electronics*, 28(1), 221-233.
31. Tsili, M.; and Papathanassiou, S. (2009). A review of grid code technical requirements for wind farms. *IET Renewable Power Generation*, 3(3), 308-332.
32. Cabrera-Tobar, A.; Bullich-Massagué, E.; Aragüés-Peñalba, M.; and Gomis-Bellmunt, O. (2016). Review of advanced grid requirements for the integration of large scale photovoltaic power plants in the transmission system. *Renewable and Sustainable Energy Reviews*, 62, 971-987.
33. Rini Ann Jerin, A.; Kaliannan, P.; and Subramaniam, U. (2017). Testing of low voltage ride through capability compliance of wind turbines - A Review. *International Journal of Ambient Energy*, (just-accepted), 1-20.
34. Photovoltaics, D.G. (2009). IEEE application guide for IEEE Std 1547™, IEEE standard for interconnecting distributed resources with electric power systems.
35. Yang, Y.; Enjeti, P.; Blaabjerg, F.; and Wang, H. (2015). Wide-scale adoption of photovoltaic energy: Grid code modifications are explored in the distribution grid. *IEEE Industry Applications Magazine*, 21(5), 21-31.
36. Yang, Y.; Wang, H.; and Blaabjerg, F. (2014). Reactive power injection strategies for single-phase photovoltaic systems considering grid requirements. *IEEE Transactions on Industry Applications*, 50(6), 4065-4076.
37. Blaabjerg, F.; Teodorescu, R.; Liserre, M.; and Timbus, A. V. (2006). Overview of control and grid synchronization for distributed power

generation systems. *IEEE Transactions on Industrial Electronics*, 53(5), 1398-1409.

38. Romero-Cadaval, E.; Spagnuolo, G.; Franquelo, L. G.; Ramos-Paja, C. A.; Suntio, T.; and Xiao, W. M. (2013). Grid-connected photovoltaic generation plants: Components and operation. *IEEE Industrial Electronics Magazine*, 7(3), 6-20.
39. Kobayashi, H. (2012). Fault ride through requirements and measures of distributed PV systems in Japan. In *Power and Energy Society General Meeting, 2012*, 1-6.
40. Ding, G.; Gao, F.; Tian, H.; Ma, C.; Chen, M.; He, G.; and Liu, Y. (2016). Adaptive DC-link voltage control of two-stage photovoltaic inverter during low voltage ride-through operation. *IEEE Transactions on Power Electronics*, 31(6), 4182-4194.
41. Prabaharan, N.; and Palanisamy, K. (2016). Analysis and integration of multilevel inverter configuration with boost converters in a photovoltaic system. *Energy Conversion and Management*, 128, 327-342.
42. Prabaharan, N.; and Palanisamy, K. (2016). A single phase grid connected hybrid multilevel inverter for interfacing photo-voltaic system. *Energy Procedia*, 103, 250-255.
43. Prabaharan, N.; and Palanisamy, K. (2016). Modeling and analysis of a quasi-linear multilevel inverter for photovoltaic application. *Energy Procedia*, 103, 256-261.